LAWRENCE
LIVERMORE
NATIONAL
LABORATORY

LLNL-PROC-646485

Influence of Growth Behavior on Laser-Induced Bulk Damage in Deuterated Potassium Di-hydrogen Phosphate (DKDP) Crystals

Z. M. Liao, R. Roussell, J. J. Adams, M. A. Norton, M. Runkel, W. T. Frenk, J. Luken, C. W. Carr

November 19, 2013

SPIE Laser Damage 2013
Boulder, CO, United States
September 22, 2013 through September 25, 2013

Disclaimer

the smallest sizes suitable for absorbing energy in sufficient density [18]. The size-dependent scaling power coefficient, b, is set to be ~3 because this is a typical value for characterizing size variation in optics contamination [19]. This implies that ADM would only need 1 parameter (N) for each $\rho(\phi)$.

3. DATA ANALYSIS

NIF has more than 200 THG optics that were cut from over 50 boules of DKDP. Usually, at least one "witness sample" (~ 5 x 5 cm square) from each boule has been damage tested using the damage probability test at LLNL (i.e. S/1 and R/1) for quality assurance and these results have been carefully recorded in an extensive database [13, 20]. When possible, more than 1 sample from a given boule was damage tested and these samples are labeled with an identifier which denotes if they were first growth (FG) or late growth (LG) material (see Fig. 1). We have analyzed over 50 different S/1 and R/1 damage test results as well as over a dozen damage density measurements (see Table 1).

Table 1. Boule samples

	Samples with identified region	**Samples with both FG and LG region**	**Samples with $\rho(\phi)$ data**
Test data set	>50	~39	~20
Number of boules	>16	~14	~13

For each sample with a damage probability test data (i.e., S/1, R/1), we used ADM to calculate the precursor defect parameters (μ_1, σ_1, μ_2, σ_2). Fig. 2a is a scatter plot of the Type 1 (linear) absorber vs. Type 2 (nonlinear) absorber for all the samples with a known growth region. Although the mean absorption value for both Type 1 and Type 2 are similar (19.7 and 19.1 respectively), Type 2 defect precursors have a larger variance than Type 1 defect precursors. Interesting, the mean of the growth regions are fairly close to each other with the FG region (μ_1=19, μ_2=20) and LG region (μ_1=21, μ_2=17) being closely related. Precursors from difference growth regions are not tightly clustered, but overlap each other; this is assumed to reflect that the variability from boule to boule is larger than the variability from growth region within the same boule. This is clearly illustrated when we restrict our plot to only one boule, LL16 (see Fig. 2b), which has 10 damage probability measurements from the FG growth region and 4 damage probability measurements from the LG growth region. Both the FG and LG defect precursors for this boule are close to the mean absorption of all the boules (see Fig. 2(a)), indicating that this boule is not an outlier. It is also apparent that the Type 2 defect absorber have more variance than the Type 1 precursor (also keeping in trend with the sample population), with LG data having less variation than FG data. It is also interesting to see clearly the Type 2 defect precursor (μ_2) decreases as the boule transitions from FG to MG to LG, which agrees with previous results that show an increasing "purity" [8] or a decrease in "emission clusters" (i.e., contaminant) [7, 9] as the boule grows. The fact that previous studies [7-9] didn't find significant difference in damage behavior in FG vs. LG also wasn't surprising from this result. Although the precursor absorption of the FG sample is larger than LG, the variance is large enough that a significant amount of testing (in our case, ~ 8 tests) would be required to demonstrate the trend, whereas previous studies typically tested only a single sample.

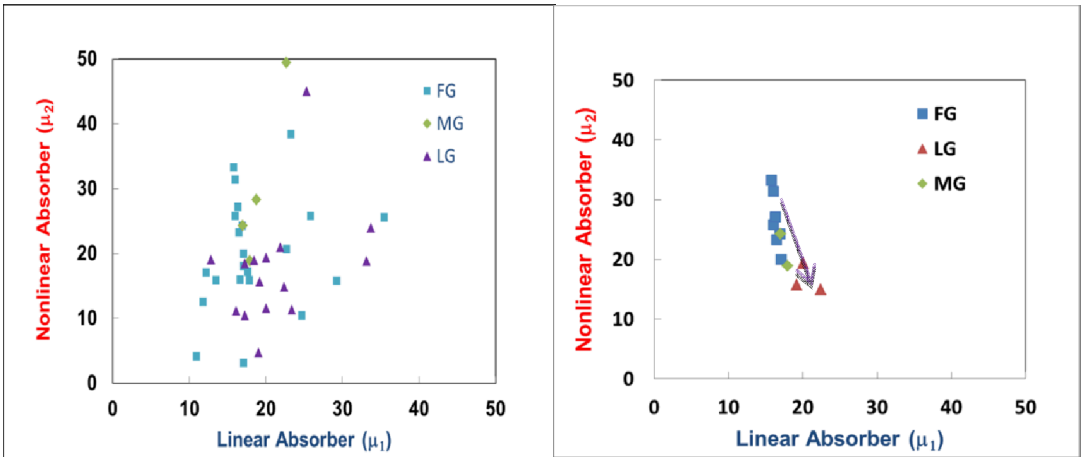

Fig. 2a. Plot of Type 1 (μ_1) vs. Type 2 (μ_2) defect precursor absorption for all data with known growth region from all boules. Fig. 2b: Plot of Type 1 (μ_1) vs. Type 2 (μ_2) defect precursor absorption from a single boule (LL16).

In order to see the possible relationship of growth region for all the boules, the data is plotted in which a vector is used to show the relationship of a given boule's FG growth region to LG growth region. In the figure, which has the same axis as Fig. 2, each boule is represented by an arrow vector whose arrow end represents the value for the LG portion of the boule, and the starting point of the vector represents the FG portion of the boule. The direction of the vector shows the boule as increasing its purity or decreasing its purity as it grows and the length of the vector denotes the degree of heterogeneity of the boule (from FG to LG). What emerges from this graph is a grouping of the boules that shows at least 2 distinct behaviors that we have labeled as Group A and B (see Fig. 3).

1. Group A consists of 8 boules that have LG Type 2 defect precursor absorption μ_2 (LG) $\leq$ 19. All of these boules have a higher Type 2 defect precursor absorption for FG vs. LG. These boules behave exactly like LL16, which we have presented in Fig. 2(b), where we have seen an increasing "purity" as the boule is grown, which is consistent with previous findings [7-9]. These boules in general have a better damage performance because of the lower Type 2 defect precursor absorption.
2. Group B consists of 6 boules that have LG Type 2 defect precursor absorption μ_2 (LG) >19. The primary difference of Group B boules in contrast to Group A boules, is that all boules have a lower Type 2 defect precursor absorption for FG vs. LG. As a result, Group B boules in general exhibit a decreasing "purity" as the boule is grown. Since these boules in general have a higher Type 2 defect precursor absorption, these boules also exhibit a poorer damage performance.

In terms of conditioning or damage performance, the boules from Group B would have the lower damage threshold, but they also would have a lower conditioning threshold. As for a fully conditioned damage threshold (which depends strongly on Type 1 defect precursor absorption), the nominal boule from Group A and B would have similar performance. An interesting observation is that unlike the Type 1 absorption value in which there is a 60-40 split with respect to increasing vs. decreasing purity (i.e., arrow pointing up or down in Fig. 3) going from FG to LG, all of the boules exhibit decreasing purity in intrinsic precursors (i.e., Type 1) except for two boules that we have identified using double lines in Fig. 3. These two boules are outliers (and also most recent growth runs) in that although they both belong to Group A, one of them has the lowest R/1 damage fluence (highest Type 1 value) and the other one has the highest R/1 damage fluence (lowest Type 1 value) of all the boules. They represent the opposite ends of the spectrum, and if we can determine what caused this difference, it might just provide the key identifier in growing better damage-resistant boules. It is clear that these correlations play an important role in the amount and kind of precursors that the boules inherit from the growth process. It was confirmed by the manufacturer of these boules after reviewing this classification that the distinction of Group A vs. Group B generally corresponds to growth parameters they have long suspected play an important role in damage performance.

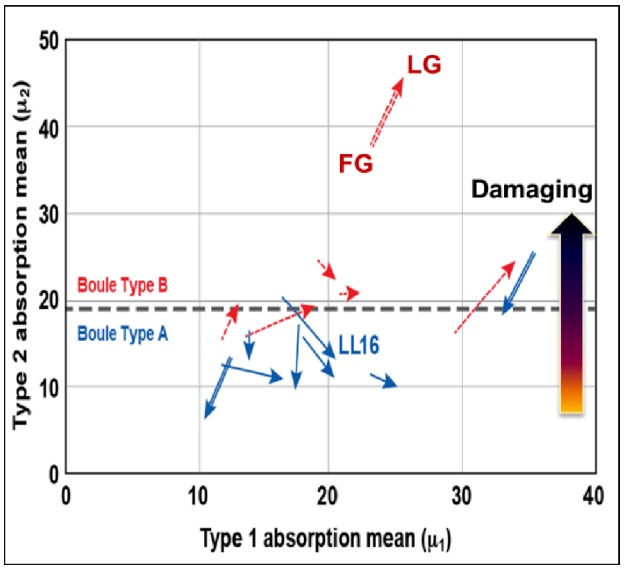

Fig. 3. Plot of Type 1 vs. Type 2 defect precursor absorption for each boule and the relationship between the FG and LG as indicated by the direction of the arrow.

Damage density $\rho(\phi)$ tests have been performed on a number of the same samples over the years at LLNL for pulse-width dependence and conditioning studies [3, 12, 21]. Although boule IDs have always been recorded, the growth regions of the samples were usually not recorded. ADM analysis using Eq. 2 to calculate the total precursor density (N) from each $\rho(\phi)$ measurement was performed for all available data. For samples that did not have growth regions identified, we found that in every case, only one set of absorption parameters from either FG or LG probability data produced $\rho(\phi)$ that fit the data; as a matter of fact, the model could not converge on a solution using the other set of absorption values. This is an important revelation that shows the self-consistency of ADM and its ability to discriminate erroneous data. Figure 4 shows a plot of calculated total precursor density N vs. Type 1 precursor absorption μ_1. There seems to be an exponential dependence between the Type 1 defect precursor absorption μ_1 and the precursor density N for Boule Type A. The first dependence (blue line) centers around data from Group A boules and other boules (marked with green triangles) that we were not able to classify because of only having damage probability data from the FG growth region (remember it is the LG Type 2 defect precursor absorption μ_2 that differentiates group A boules from group B). The four data points from Type B boules in Fig. 4 are closely clustered so that it is impossible to draw any conclusion as to whether or not the dependence of N is constant, linear, or exponential from that data alone. However, in light of the strong exponential dependence of the data from the Type A boules, we argue that the Type B data should follow a similar trend (red dashed line).

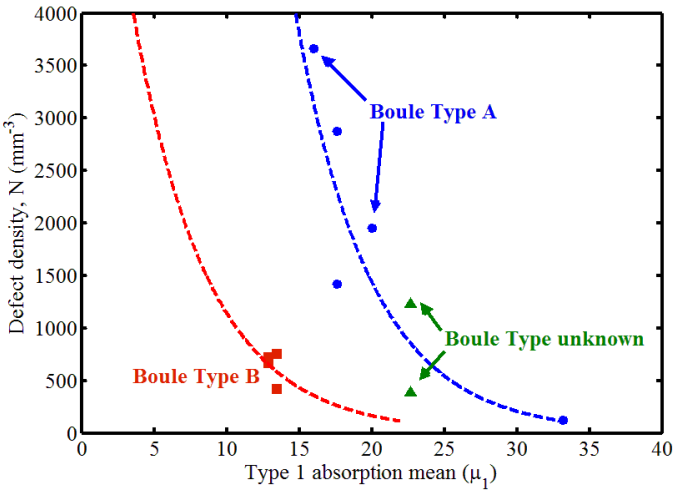

Fig. 4. Type 1 defect precursor absorption (μ_1) vs. precursor density N for Group A boules (data – circular blue, fit blue line) and Group B boules (data – red square, fit red line). Data from ungrouped boules (lack of LG data) were marked as green triangles.

4. EXPERIMENTAL VERIFICATION

As discussed in the earlier section, damage probability data is adequate for quality assurance or relative comparison, but it is not as useful in damage prediction in managing an optic's lifetime. Operational limits on laser system would have a specification that sets limits on the number of damage sites or the maximum size of damage sites. As a result, it is not practical to set the operation of a laser using the damage probability data; a 10% damage probability does not correlate to the actual number of damage initiations. Furthermore, although R/1 damage probability data can help provide the threshold for an optimal (i.e., fully) conditioned damage sample, it is difficult to extract the consequence of conditioning ramps or the number of damage initiations if the sample is only partially conditioned.

An optimal conditioning protocol can be calculated based on the results of this study. For example, given the crystal's boule type (i.e. Type A or Type B, gather from the probability of damage test data), a conditioning protocol to allow the laser system to operate at 8 J/cm^2 at 3ω using a 5-ns flat-in-time (FIT) pulse without exceeding a given damage limit can be calculate. ADM is able to calculate an optic's damage density ($\rho(\phi)$) as a function of operating fluence and conditioning fluence (see Eq. 3) with precursor parameters (μ_1, μ_2) and total precursor density, which is now a function of μ_1 and boule type (see Eq. 5). The expected number of initiations X that a laser shot can cause on a crystal can then be calculated as

$$\left\langle X(\phi_{OP},\phi_C)\right\rangle = V\cdot\int \rho(\phi_{OP};\phi_C)\cdot f(\phi;\phi_{OP},\phi_\sigma)\cdot d\phi \qquad (4)$$

with ϕ_{OP} being the mean operating fluence, ϕ_σ being the standard deviation of the damage fluence, ϕ_C being the conditioning fluence, and V being the volume of the crystal. The fluence is assumed to be from a 3-ns Gaussian—for other pulse shapes, an equivalent conversion factor would need to be calculated [22, 14]. The first term inside the integral is the calculated conditioned $\rho(\phi_{OP};\phi_C)$ (see Eq. 3) using the Type 1 and Type 2 defect parameters from damage probability test data (S/1, R/1) and the conditioned fluence ϕ_C (which modifies the Type 2 defect parameter) to which the optic has been exposed [14]. The second term in the integral is the laser fluence distribution, which for most laser

systems can be modeled as having a Gaussian (or Rician) fluence distribution with a mean fluence ϕ_{OP} and a standard deviation ϕ_σ that is directly related to beam contrast [23]. For simplicity, we will assume that the conditioning laser fluences are uniform and that the current shot has a fixed contrast of 10%. As a result, we can now calculate the conditioning matrix (i.e., conditioning map), which is the expected number of initiation sites as a function of operating mean fluence (ϕ_{OP}) and conditioned fluence (ϕ_C).

Recently, we have used ADM to calculate the optimal shot sequence to condition crystals online in NIF (~ 40 x 40 cm^2) to ~ 8 J/cm^2. The previous protocol was conservatively based on a damage probability test and required 9 shots to reach 8 J/cm^2. ADM is used to calculate the conditioning map using data from the worst boule from Group B, which has defect parameters similar to the boule on the very top of the graph in Fig. 4, also one of the lowest damage resistant boules in the study. Figure 5a shows the number of expected initiations using contours in log value as a function of conditioned fluence (ϕ_C) in the horizontal axis and operating fluence (ϕ_{OP}) in the vertical axis. If the specification is the total initiation sites, $X_{max} = 10^5$ sites, then an optimal conditioning sequence can be individually calculated for each boule (see solid red line). The conditioning sequence is optimized by maximizing the damage fluence of each shot (vertical axis) given the current conditioning fluence (horizontal axis), so that the accumulated initiation sites (X_1+ $X_{2+}..X_n$ where X_n is the number of initiations at the n^{th} shot including the desired operating fluence shot) are kept below X_{max} until the desired operating fluence is achieved. In Fig. 5b, the ADM project conditioning protocol (which has one shot added as a system margin to account for shot to shot laser fluctuation) is carried out (see current shot in Fig. 5b). In comparison, the previous protocol would require 9 shots to condition the optic (see Fig. 5b), the online damage inspection result have indicated that both of the optics have passed the damage criterion, but with the new ADM predicted conditioning protocol, the laser facility was able to reduce nearly half the number of shots.

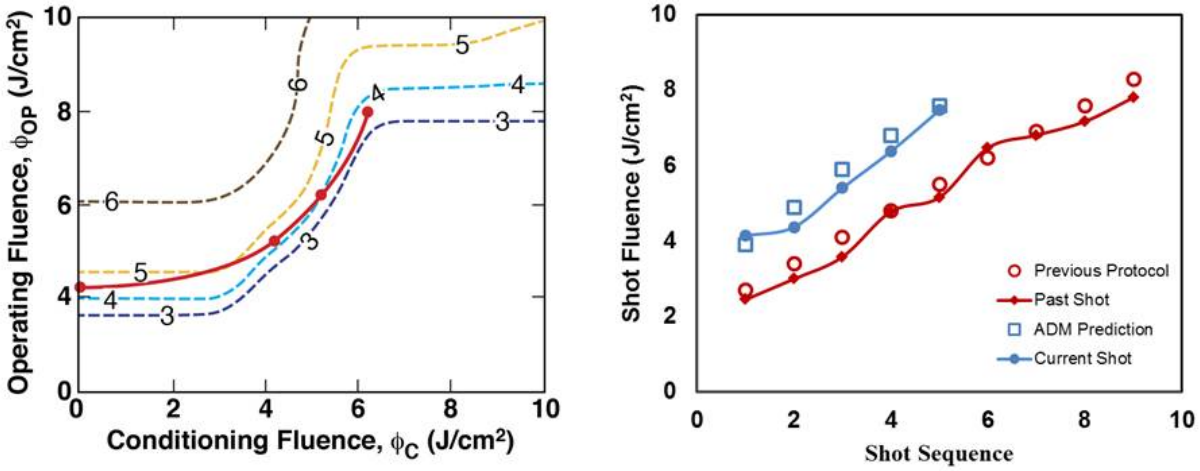

Fig. 5a. Contour plot of the conditioning map showing the number of damage initiations (in log units) for a the worst boule from Group B and the optimal conditioning sequence to reach 8 J/cm^2 is shown in red solid line. Fig. 5b. Conditioning shot sequence for previous protocol (9 shots) and current ADM predict protocol (5 shots)

In addition, we have also used ADM to predict the optimal conditioning sequence for a smaller aperture laser, the Optical Science Laser (OSL, ~ 1 cm^2) with criterion of no damage initiation allowed. The test sample was from boule LL16, which is a nominal boule for Group A. A different sub-aperture of the sample was then shot with a variety of conditioning sequence; some adhere to the ADM predicted optimal conditioning sequence while others exceed the conditioning protocol at some shot sequences. The results (see Fig. 7) of the experiment indicate that only those shots that exceed the ADM predicted conditioning protocol yield damages.

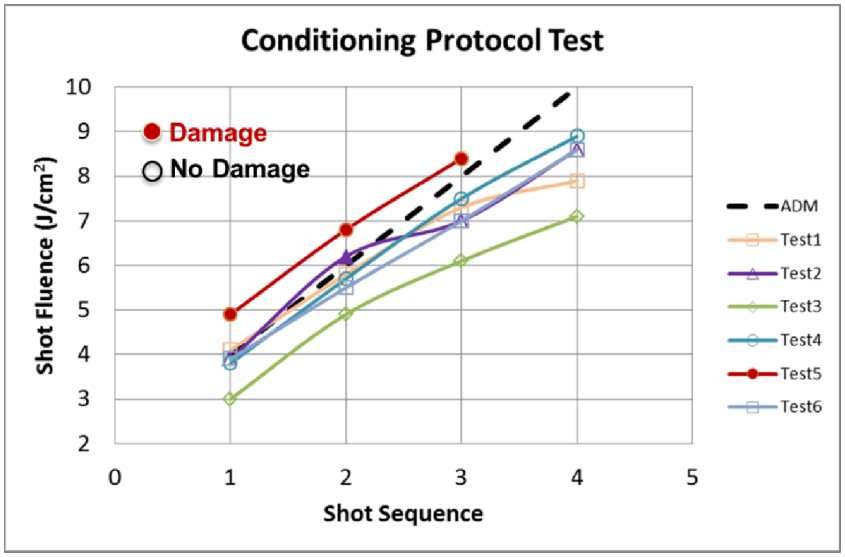

Fig. 7. ADM predicted conditioning protocol for no initiation and various test conditioning protocols (1-6). Open symbol shot fluence indicated no damage observed on that shot, closed symbol shot fluence indicated damage observed on that shot. ADM prediction is successfully verified as only shots that exceed ADM prediction yield damage.

5. CONCLUSION

ADM was used to analyze damage test results from over a dozen DKDP boules to investigate variations of defect populations from boule to boule as well as different growth regions within a boule. Large variations of defect populations of both types were found from boule to boule, this variation was larger than the variation of different growth region within the same boule. However, within the same boule, there does seem to be a progressive evolution of defect precursor transition from first growth to the late growth region. Furthermore, survey of dozens of boules showed two distinct groupings of the boules with this grouping also playing a critical role in determining the relationship between the linear precursor defect and the total defect precursor density. This finding has been used to successfully predict the optimal conditioning protocol for both large aperture lasers such as NIF as well as smaller aperture lasers such as OSL.

REFERENCES

[1] P. Wegner, J. Auerbach, T. Biesiada, S. Dixit, J. Lawson, J. Menapace, T. Parham, D. Swift, P. Whitman, and W. Williams, "NIF final optics systems: frequency conversion and beam conditioning," Proc. SPIE **5341**, 180 (2004).

[2] J. Swain, S. Stokowski, D. Milam, and F. Rainer, "Improving the bulk laser damage resistance of potassium dihydrogen phosphate crystals by pulsed laser irradiation," Appl Phys Lett. **40**, 350 (1982).

[3] J. J. Adams, C. W. Carr, M. D. Feit, A. M. Rubenchik, M. L. Spaeth, and R. P. Hackel, "Pulse length dependence of laser conditioning and bulk damage in KD_2PO_4," Proc. SPIE **5647**, 265 (2004).

[4] M. Runkel, K. Neeb, M. Staggs, J. Auerbach, and A. Burnham, "The results of raster scan laser conditioning studies on DKDP triplers using Nd:YAG and excimer lasers," Proc. SPIE **4679**, 348 (2001).

[5] M. Runkel and A. K. Burnham, "Difference in bulk damage probability distributions between tripler and z-cuts of KDP and DKDP at 355nm," Proc. SPIE **4347**, 408 (2000).

[6] A. K. Burnham, M. Runkel, R. A. Hawley-Fedder, M. L. Carman, R. A. Torres, and P. K. Whitman, "Low-temperature growth of DKDP for improving laser-induced damage resistance at 350nm," Proc. SPIE **4347**, 373 (2000).

[7] S. G. Demos, M. Staggs, M. Yan, H. B. Radousky and J. J. De Yoreo, "Investigation of optically active defect clusters in KH_2PO_4 under laser photoexcitation," J. Appl. Phys. **85**, 3988 (1999).

[8] M. Yan, R. Torres, M. Runkel, B. Woods, I. Hutcheon, N. Zaitseva, and J. DeYoreo, "Investigation of impurity and laser-induced damage in the growth sectors of rapidly grown KDP crystals," Proc. SPIE **2966**, 11 (1997).
[9] M. Pommies, D. Damiani, B. Bertussi, J. Capoulade, H. Piombini, J. Y. Natoli, and H. Mathis, "Detection and characterization of absorption heterogeneities in KH_2PO_4 crystals," Opt. Comm. **267** 154 (2006).
[10] R. A. Negres, N. P. Zaitseva, P. DeMange, and S. G. Demos, "An expedited approach to evaluate the importance of different crystal growth parameters on laser damage performance in KDP and DKDP," Proc. SPIE **6403**, S4031 (2007)
[11] M. Runkel, M. Yan, J. De Yoreo, and N. Zaitseva, "The effect of impurities and stress on the damage distributions of rapidly grown KDP crystals," Proc. SPIE **3244**, 211 (1997).
[12] C. W. Carr, M. D. Feit, M. C. Nostrand, and J. J. Adams, "Techniques for qualitative and quantitative measurement of aspects of laser-induced damage important for laser beam propagation," Meas. Sci. Technol. **17**, 1958 (2006).
[13] J. Adams, J. A. Jarboe, M. Feit, and R. P. Hackel, "Comparison between S/1 and R/1 tests and damage density vs. fluence (rho(phi)) results for unconditioned and sub-nanosecond laser-conditioned KD_2PO_4 crystals," Proc. SPIE **6720**, 72014 (2008).
[14] Z. M. Liao, M. L. Spaeth, K. Manes, J. J. Adams, and C. W. Carr, "Predicting laser-induced bulk damage and conditioning for deuterated potassium dihydrogen phosphate crystals using and absorption distribution model," Opt. Lett., **35**, 2538 (2010).
[15] M. Spaeth, "Absorption Distribution Model," LLNL Internal Presentation, (2007).
[16] Z. M. Liao, R. Roussel, J. J. Adams, M. Runkel, W. T. Frenk, J. Luken, and C. W. Carr, "Defect population variability in deuterated potassium dihydrogen phosphate crystals," Opt. Mat. Exp., **2**, 1612 (2012).
[17] C. W. Carr, J. D. Bude, and P. DeMange, "Laser-supported solid-state absorption fronts in silica," Phy. Rev. B. **82**, 184304 (2010).
[18] M. D. Feit and A. M. Rubenchik,"Implications of nanoabsorber initiators for damage probability curves, pulselength scaling and laser conditioning," Proc. SPIE **5273**, 74 (2003).
[19] J. B. Trenholme, A. M. Rubenchik, and M. D. Feit, "Size-selection initiation model extended to include shape and random factors," Proc. SPIE **5991**, X9910 (2005).
[20] M. Runkel, M. Yan, J. De Yoreo, and N. Zaitseva, "The effect of impurities and stress on the damage distributions of rapidly grown KDP crystals," Proc. SPIE **3244**, 211 (1997).
[21] M. Runkel, J. Bruere, W. Sell, T. Weiland, D. Milam, D. Hahn, and M. Nostrand, "Effects of pulse duration of bulk laser damage in 350-nm raster-scanned DKDP," Proc. SPIE **4392,** 405 (2002).
[22] C. W. Carr, J. B. Trenholme, and M. L. Spaeth, "Effect of temporal pulse shape on optical damage," Appl. Phy. Lett. **90**, 041110 (2007).
[23] Z. M. Liao, J. Huebel, and J. Trenholme, "Modeling max-of-N fluence distribution using measured shot-to-shot beam contrast," Applied Optics **50**, 3547 (2011).

ACKNOWLEDGEMENT

The author would like to acknowledge helpful discussions and edits with Chris Stolz, Tayyab Suratwala, and Jeff Bude. This work was performed under the auspices of the U. S. Department of Energy by Lawrence Livermore National Laboratory under Contract DE-AC52-07NA27344. (LLNL-JRNL-646485)